Colloids and Surfaces B: Biointerfaces 69 (2009) 99–104

Contents lists available at ScienceDirect

Colloids and Surfaces B: Biointerfaces

journal homepage: www.elsevier.com/locate/colsurfb

Fabrication of the nanogapped gold nanoparticles film for direct electrical detection of DNA and EcoRI endonuclease

Chengjun Wang[a,b], Jiarui Huang[a], Jin Wang[a], Cuiping Gu[a], Junhai Wang[a], Buchang Zhang[b], Jinhuai Liu[a,*]

[a] Institute of Intelligent Machines, Chinese Academy of Sciences, Anhui 230031, People's Republic of China
[b] School of Life Science, Anhui University, Anhui 230039, People's Republic of China

ARTICLE INFO

Article history:
Received 8 July 2008
Received in revised form
14 November 2008
Accepted 14 November 2008
Available online 24 November 2008

Keywords:
Nanogapped gold nanoparticles film
In situ seeding growth
DNA
EcoRI endonuclease
Electrical detection

ABSTRACT

In situ seeding growth of gold nanoparticles (AuNPs) by the reaction of $HAuCl_4$ and NH_2OH has been employed in the fabrication of the nanogapped AuNPs film for direct electrical detection of DNA hybridization and DNA cleavage by EcoRI endonuclease. The distance between neighboring gold nanoparticles is less than the length of the probe DNA, implying that the DNA strand could bridge the AuNPs to provide an electron tunneling path between microelectrodes. The double-stranded DNA (dsDNA) formed by hybridization of probe and target DNA is detected by current–voltage (*I–V*) curve measurements. When dsDNA is cleaved by restriction endonuclease EcoRI, the electron tunneling path can be cut off, which is reflected from the different slopes of *I–V* curves between dsDNA and dsDNA cleavage by EcoRI in the label-free electrical measurements. The novel and simple method of fabricating the nanogapped AuNPs film by in situ seeding growth could provide a promising bioanalytical platform for studying both DNA–DNA and DNA–protein interactions.

1. Introduction

Gene engineering plays an important role in the field of modern life science. It generates a growing demand, in particular for tests of DNA hybridization and DNA–protein interactions. The detection of DNA hybridization becomes increasingly important for applications including point-of-care diagnostics, environmental monitoring and forensic analysis. Although DNA had been regarded as insulator, based on charge transfer via stacked aromatic bases (π–π stacking) in DNA molecule, the DNA electrical conductivity was proposed [1,2]. Compared to some other traditional technologies such as optical [3], electrochemical [4] and gravimetric [5] methods, electrical detection of DNA [6–8] has been recognized as a promising technique because of its straightforwardness in signal interfacing and processing as well as in the integration of a DNA microarray system. On the other hand, DNA–protein interactions play important roles in life processes, such as DNA replication, transcription and repair. EcoRI endonuclease is among the simplest site-specific DNA enzymes and it is useful for the study of the mechanisms governing the interaction of such proteins with DNA [9,10]. The enzyme functions as a homodimer of a 31-kDa polypeptide [11], and introduces two staggered, single-strand scissions into the symmetric recognition sequence, 5′-GAATTC-3′ [12]. Up to date, many studies about DNA–EcoRI interaction have been performed by atomic force microscopy [13], cantilevers [14], optical detection [15], gel electrophoresis [16] and electrochemical detection [17]. However, few works about the electrical detection of DNA–EcoRI interaction have been done.

The development in the field of nano- and molecular electronics depends greatly on the ability to fabricate nanometer-sized gaps between electrodes [18,19]. It is difficult to fabricate structures smaller than 10 nm with current lithography methods, and even more challenging to build the gap which should be equal or slightly less than the length of the biomolecule. In this connection, precise control of the electrode gap in nanometer range is a crucial factor for DNA electrical detection. As a gap adaptor, the gold nanoparticle which has been widely applied in DNA sensing [20–22], was used to address this issue. Mirkin's group reported that AuNPs were captured in between micrometer-gapped electrodes by the hybridization of DNA strands. Then silver deposition facilitated by the gold nanoparticles bridged the gap and led to electrical detection of DNA indirectly [23]. Shiigi et al. [24] developed another method, i.e., utilizing alkylthiol as a cross-linker to fabricate a nano-gapped gold particle film consisting of gold nanoparticle–alkylchain–gold nanoparticle repeated sequences. Tsai et al. [25] built up the second layer of AuNPs using hexanedithiol as a cross-linker and detected the electrical signal of DNA strands immobilized on self-assembled multilayer AuNPs.

* Corresponding author. Tel.: +86 551 5591142; fax: +86 551 5592420.
E-mail address: jhliu@iim.ac.cn (J. Liu).

0927-7765/$ – see front matter © 2008 Elsevier B.V. All rights reserved.
doi:10.1016/j.colsurfb.2008.11.008

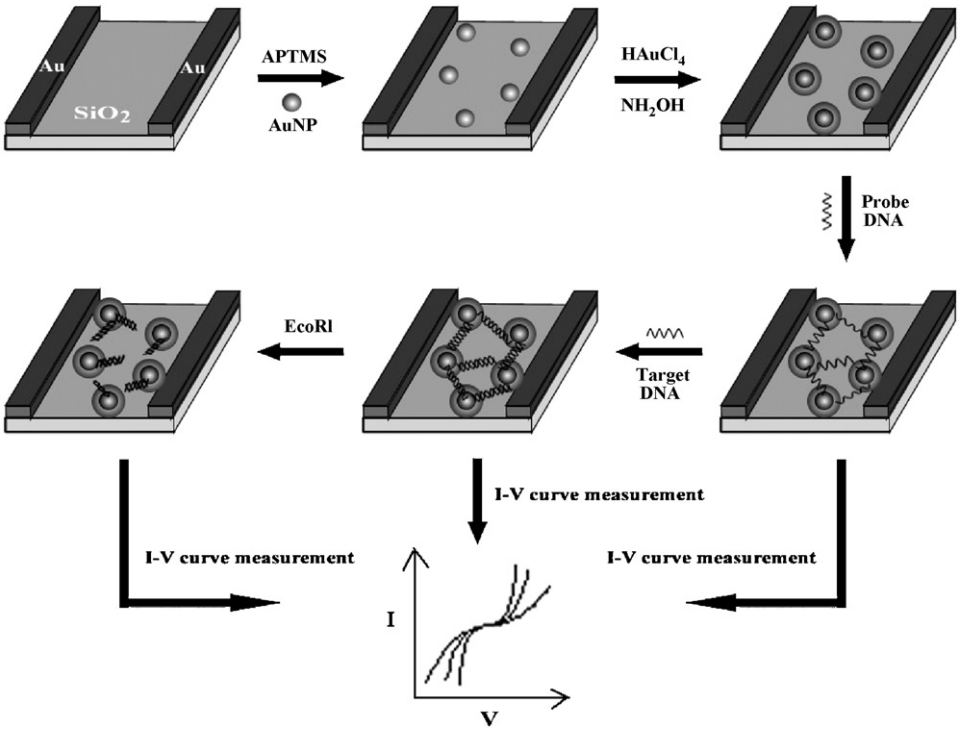

Fig. 1. Schematic illustration of the nanogapped AuNPs film fabricated by seeding growth of gold nanoparticles for electrical detection of DNA hybridization and dsDNA cleavage by EcoRI.

Compared to the approaches mentioned above, a novel and simple method of fabricating the nanogapped gold nanoparticles film by in situ seeding growth of AuNPs for electrical detection of DNA is demonstrated in this paper (Fig. 1). Using the one-step reaction of $HAuCl_4$ and NH_2OH, the distance between neighboring gold nanoparticles is mostly less than the length of the probe DNA, so that the DNA strand could bridge the AuNPs to provide an electron tunneling path between microelectrodes. The different electrical signals between single-stranded DNA (ssDNA) and double-stranded DNA (dsDNA) could be observed clearly. Hence, the method represents a rapid and effective fabrication of the nanogapped AuNPs film for label-free and direct electrical detection of DNA. Furthermore, dsDNA cleavage by EcoRI endonuclease is studied using the nanogapped AuNPs film by electrical detection. The dsDNA cleavage by EcoRI endonuclease is studied easily and directly by the *I–V* curve measurement. Therefore, the new method has been developed to monitor not only DNA hybridization but also DNA–protein interactions.

2. Materials and methods

2.1. Materials and reagents

FastDigest™ Restriction Enzyme EcoRI and 10 × FastDigest™ buffer were purchased from Fermentas International Inc. (Canada). Hydroxylamine hydrochloride ($NH_2OH{\cdot}HCl$, Sinopharm Chemical Reagent Co., Ltd., China) and HAuCl4 (Sinopharm Chemical Reagent Co., Ltd., China) were used for the seeding growth of AuNPs. 3-Aminopropyl-trimethoxysilane (APTMS) was purchased from Sigma–Aldrich and trisodium citrate was obtained from Sinopharm Chemical Reagent Co. (Shanghai, China). Millipore Milli-Q water ($18.2\ M\Omega\ cm^{-1}$) was used in all experiments.

ssDNA oligonucleotides were synthesized by Shanghai Sangon Biological Engineering Technology and Services Co., Ltd. (Shanghai, China). Thiolated probe DNA1 and complementary target DNA2 contained two recognition sequences for the ECoRI restriction endonuclease. Control thiolated DNA3 and complementary target DNA4 were designed without specific recognition site of the ECoRI endonuclease. Sequences of these DNA were shown in Table 1. All of them were dissolved into TE buffer solution (10 mM Tris–HCl, 1 mM EDTA, 1 M NaCl, pH 7.5) before used.

2.2. Fabrication of single-layered AuNPs

AuNPs were prepared using the citrate reduction method introduced by Turkevitch et al. [26] and further developed by Frens [27]. 1 mL of 1% $HAuCl_4$ was added into 100 mL Milli-Q water and heated until boiling. Then 4 mL 1% trisodium citrate at room temperature was added while stirring, the solution underwent a series of color changes and 15 min later it turned wine red. The field-emission scanning electron microscope (FE-SEM, Sirion 200 FET) micrograph revealed that the average diameter of AuNPs was 15 ± 3 nm.

The interdigital gold microelectrode (60 nm gold on 10 nm titanium) with 8 μm gap was fabricated by electron beam lithography on a SiO_2 wafer (Fig. 2A). Before assembling the single layer of AuNPs (s-AuNPs) in the gap between microelectrodes, the substrate was immersed in acetone solution for 2 h, and then was immersed in the piranha solution (H_2SO_4:H_2O_2 = 3:1, v/v) for 10 min, followed by rinsing with Milli-Q water. Subsequently, it was treated with 1 mM APTMS of ethanol solution for 2 h at room temperature. One end of the APTMS is to silanize the substrate surface while the thiol end of the APTMS is used to bind the AuNPs. The substrate was rinsed with ethanol and dried under a stream of N_2. Then it

Table 1
Sequences of the four DNA strands used in this experiment.

Name	Sequence
DNA1	5′-HS-ATG CTG CTC TAC *GAA TTC* ATA GCG TAC G*GA ATT C*TG GCC T-3′
DNA2	5′-AGG CCA *GAA TTC* CGT ACG CTA T*GA ATT C*GT AGA GCA GCA T-3′
DNA3	5′-HS-ATG CTG CTC TAC ATC GTA ATA GCG TAC GAT CGT ATG GCC T-3′
DNA4	5′-AGG CCA TAC GAT CGT ACG CTA TTA CGA TGT AGA GCA GCA T-3′

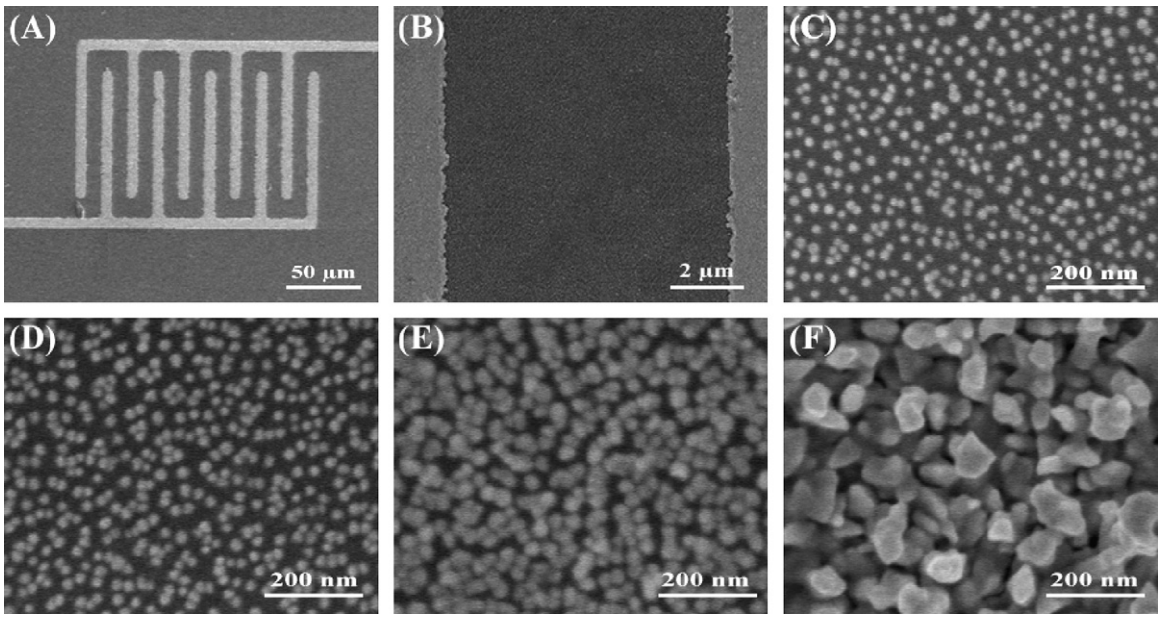

Fig. 2. FE-SEM images of the electrodes: (A) the interdigitated microelectrode used in the experiment; (B) assembled with s-AuNPs after the silanization treatment; (C) the s-AuNPs before seeding growth between electrodes; (D) the sg-AuNPs between electrodes after in situ seeding growth of 1 min; (E) the sg-AuNPs between electrodes after growth of 2 min; and (F) the sg-AuNPs between electrodes after growth of 3 min.

was immersed in the prepared AuNPs solution for 8 h, rinsed with Milli-Q water and dried with N_2.

2.3. In situ seeding growth of gold nanoparticles

The solution for AuNPs seeding growth was prepared by mixing together 0.01% $HAuCl_4$ and 0.4 mM $NH_2OH{\cdot}HCl$ freshly. The substrate was placed in a clean Pyrex dish followed by the addition of the seeding growth solution. The reaction was allowed to proceed for 2 min at 28 °C while continuously agitating the Pyrex dish to swirl the solution over the substrate surface. After removal, the surface was immediately washed with Milli-Q water, dried under a stream of N_2. The distance between AuNPs was dependent on the total reaction time, which ensured the controllability of the distance. As the reaction time increased, the distance between AuNPs was decreased. The seeding grown gold nanoparticles (sg-AuNPs) on the substrate surface were monitored with the scanning electron microscope.

2.4. DNA probe immobilization and hybridization

After the microelectrode was immobilized with monolayer of sg-AuNPs, thiolated probe DNA1 was then assembled on the surface of sg-AuNP by Au–S bond. 5 μL solution of 10 μM probe DNA1 in TE buffer (pH 7.5) was added to the substrate and kept it in a humid environment at 35 °C for 1 h. Then the substrate was rinsed with TE buffer to remove the unlinked and weakly adsorbed probe DNA1 and dried with N_2.

5 μl TE buffer involving 100 nM target DNA2 which was complemented to the probe DNA1 strand was pipetted onto the DNA1 modified substrate, and proceeding for 2 h at 37 °C. Hybridization occurred between DNA1 and DNA2 in the solution to form dsDNA on the surface of AuNPs. Then the substrate was rinsed with TE buffer to remove the unbound target DNA2 and dried with N_2.

The microelectrode, which had s-AuNPs before seeding growth, was immobilized with probe DNA1 and hybridized with target DNA2 in order to be compared with the one containing sg-AuNPs.

2.5. Enzyme cleavage of surface-immobilized dsDNA

The Fermentas FastDigest™ Restriction Enzyme EcoRI, which was specifically formulated to cleave DNA in just 5 min, was used in the experiment. The digestion media, which was prepared using 1 μL of EcoRI (1 FDU/μL) and 2 μL enzyme reaction buffer (10 × FastDigest™ buffer), was placed on the dsDNA oligonucleotides immobilized microelectrode and incubated in a dark, humid environment for 5 min at 37 °C. Then the microelectrode surface was washed with Milli-Q water, dried under a stream of N_2.

Control probe DNA3 and complementary target DNA4 which were designed without specific recognition site of the EcoRI endonuclease were used under the same treatment. Enzyme reaction buffer was placed on the dsDNA immobilized microelectrode only as a control experiment.

2.6. Electrical measurements

The current–voltage (I–V) curve was measured by a picoammeter voltage sourcemeter (Keithley 6487, USA) with a bias voltage from −1.5 V to 1.5 V. All electrical measurements were performed under the N_2 condition using a Faraday copper cage at 25 °C.

3. Results and discussion

3.1. Characterization the nanogapped AuNPs film between microelectrodes

After performing the s-AuNPs between microelectrodes, the in situ growth of gold nanoparticles was achieved by treatment with a freshly prepared solution containing $HAuCl_4$ and $NH_2OH{\cdot}HCl$. The increase of the size of AuNPs in the catalytic growth process could cause the change of the optical or electronic properties of AuNPs [28]. The catalytic growth of AuNPs has been employed in several DNA analytical methods [23,29–32]. The seeding approach is an excellent route to enlargement of gold nanoparticles. Natan's group had used hydroxylamine to enlarge gold nanoparticles in

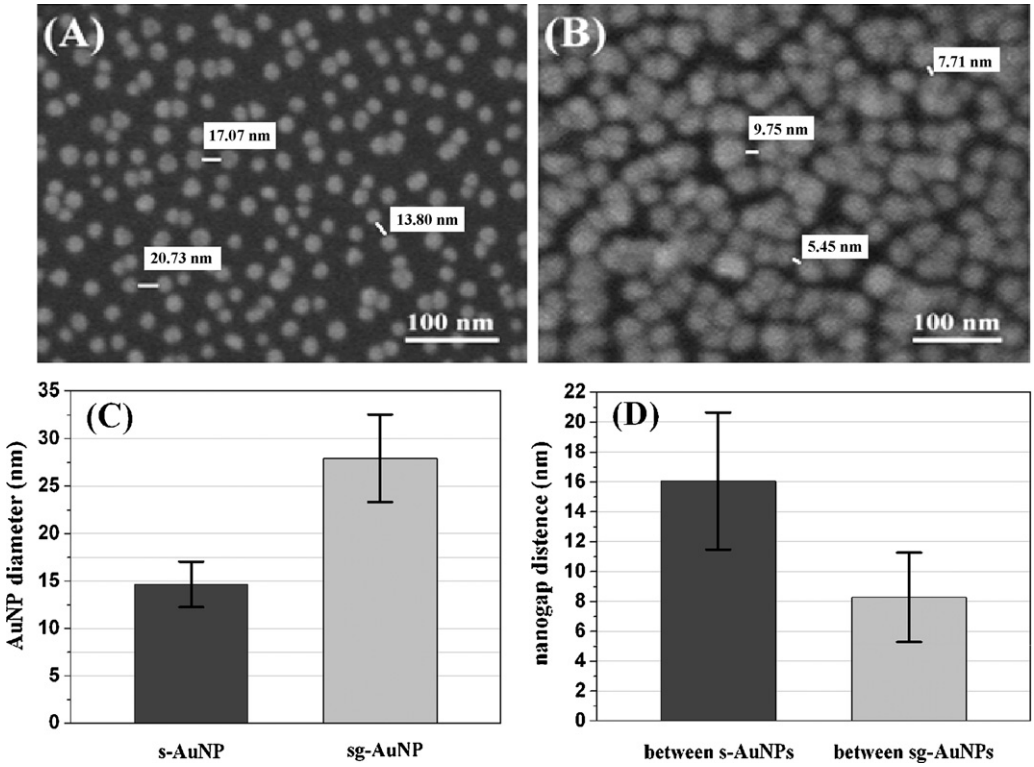

Fig. 3. SEM imaging analysis of gold nanoparticles and the distance between AuNPs: (A) close-up view of the s-AuNPs between electrodes before seeding growth; (B) close-up view of the sg-AuNPs between electrodes after 2 min seeding growth; (C) the nanoparticle diameters of s-AuNP and sg-AuNP (50 analyzed nanoparticles); (D) the nanogap distance between AuNPs before and after 2 min seeding growth (50 analyzed nanogaps).

solution [28,33] and form conductive gold films from particles immobilized on a substrate [34]. On the basis of the colloidal Au surface-catalyzed reduction of Au^{3+} by NH_2OH, a method for enlargement of colloidal gold nanoparticles called "seeding" is described herein. While NH_2OH is thermodynamically capable of reducing Au^{3+} to bulk metal, the reaction is dramatically accelerated by Au surfaces. As a result, no new particle nucleation occurs in solution, and all added Au^{3+} participates in producing larger particles [28].

The growth of gold nanoparticles between microelectrodes is conveniently observed by FE-SEM. As Fig. 2B and C illustrate, the s-AuNPs are uniformly deposited in the gap between microelectrodes with a silanization treatment. However, the distance between neighboring s-AuNPs is usually more than 13 nm (Fig. 3A) in comparison with the length (13 nm) of the DNA strand (40 base pairs) in the present experiment. It is suggested that the DNA strand cannot bridge s-AuNPs due to the long relative distance between neighboring s-AuNPs. Fig. 2D displays the sg-AuNPs between microelectrodes after 1 min growth. The size of sg-AuNP is increased a very little, and the distance between neighboring sg-AuNPs is almost not decreased. After 2 min seeding growth, as shown in Fig. 2E, the size of the sg-AuNP is increased (from 15 ± 3 to 28 ± 4 nm; Fig. 3C) and the distance between sg-AuNPs is decreased (from 16 ± 5 to 8 ± 3 nm; Fig. 3D). The distance between neighboring sg-AuNPs is less than 10 nm (Fig. 3B). Hence, the DNA strand can bridge the neighboring sg-AuNPs to provide an electron tunneling path between microelectrodes. Fig. 2F shows the sg-AuNPs after 3 min growth, the sg-AuNPs become too large, so that the neighboring sg-AuNPs join together to form the electron tunneling path between microelectrodes. In order to control the distance less than 10 nm so that the DNA strand can bridge the neighboring sg-AuNPs, the gold nanoparticles with the growth time of 2 min was chosen to fabricate the nanogapped AuNPs film.

3.2. Electrical detection of DNA using the AuNPs film

Two interdigital gold microelectrodes containing s-AuNPs and sg-AuNPs film, respectively, were used to detect DNA hybridization by *I–V* measurements. Fig. 4A shows *I–V* curves of s-AuNPs before growth between microelectrodes. The curves a, b, and c represent *I–V* responses of bare s-AuNPs, s-AuNPs with ssDNA (probe DNA1), and s-AuNPs with dsDNA, respectively. When the thiolated probe DNA1 is immobilized on the s-AuNPs, the electric current of s-AuNPs with ssDNA is higher than the current of bare s-AuNPs (curves a and b). However, the magnitude and slope of the curves b and c are very close, which implies that there is no electrical signal difference between ssDNA and dsDNA. The distance between neighboring s-AuNPs is more than 13 nm, whereas the length of the DNA strand is 13 nm. Therefore the DNA strand cannot bridge the neighboring s-AuNPs to form an electron tunneling path. No significant electrical difference between ssDNA and dsDNA with s-AuNPs in *I–V* measurements can be observed.

From above *I–V* measurements, it is concluded that the s-AuNPs film cannot detect the 40 bp DNA because the distance neighboring s-AuNPs is more than the length of the DNA strand. The *I–V* measurements for sg-AuNPs after 2 min seeding growth are shown in Fig. 4B. Compared Fig. 4A with B, the current magnitude of sg-AuNPs is significantly higher than that of s-AuNPs, which could be ascribed as the in situ seeding growth of s-AuNPs providing more chances for electrons to tunnel between microelectrodes. Additionally, as shown from curves a and c, bare sg-AuNPs have the lowest electric current, whereas sg-AuNPs with ds-DNA have the highest electric current. As mentioned above, the distance between two neighboring sg-AuNPs is less than 10 nm after the seeding growth of s-AuNPs. Thus, the free end of a DNA string immobilized on one AuNP can lie on a random neighboring AuNPs. The electron can flow through the ss-DNA and nanoparticles so as to form an electron tunneling path between microelectrodes. The neighboring

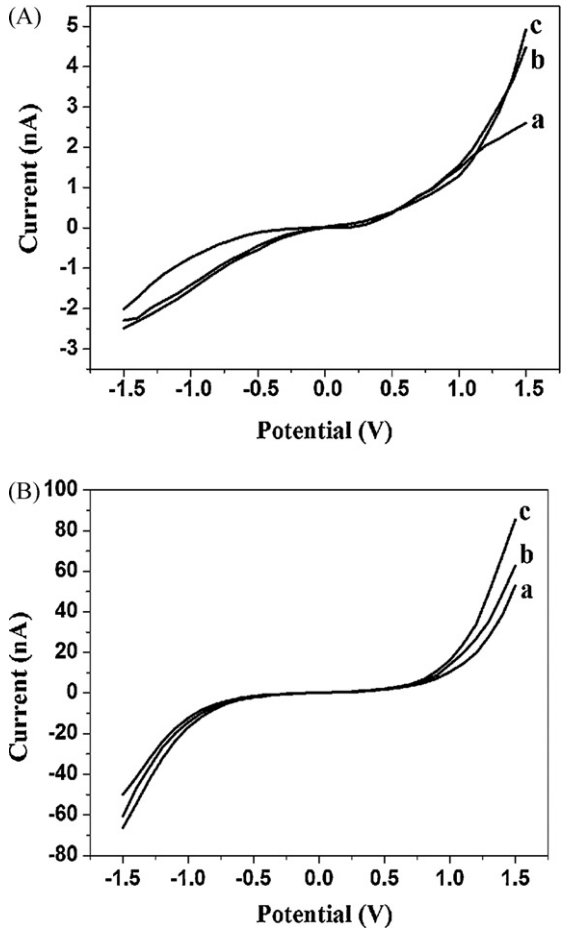

Fig. 4. Electrical detection of DNA using different AuNPs films: (A) *I–V* curves of s-AuNPs: (a) bare s-AuNPs, (b) s-AuNPs with ss-DNA, (c) s-AuNPs with ds-DNA; (B) *I–V* curves of sg-AuNPs: (a) bare sg-AuNPs, (b) sg-AuNPs with ss-DNA and (c) sg-AuNPs with ds-DNA.

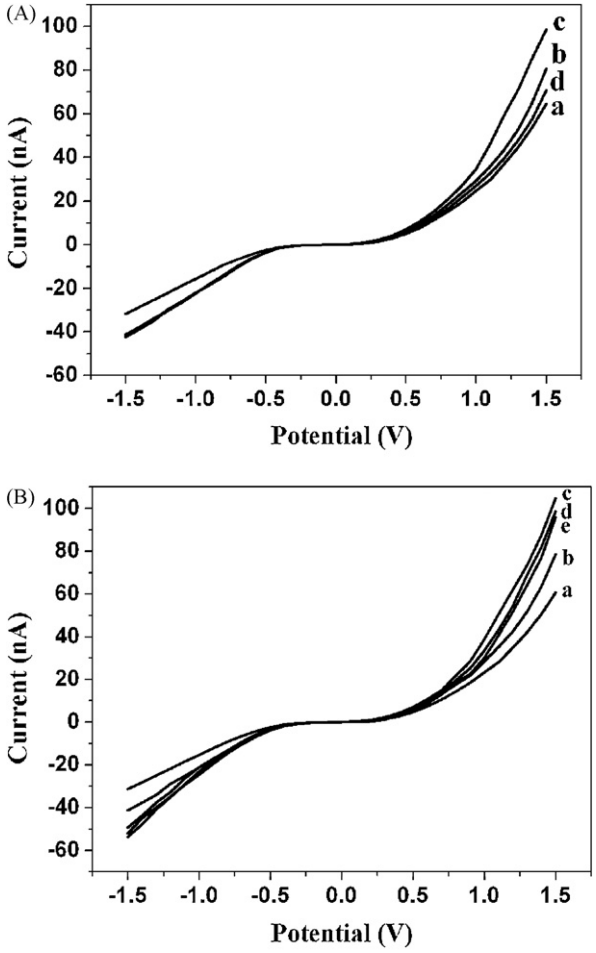

Fig. 5. Electrical detection of DNA–EcoRI interaction using the sg-AuNPs film: (A) *I–V* measurements for dsDNA cleavage by EcoRI using the sg-AuNPs film: (a) bare sg-AuNPs, (b) sg-AuNPs with ss-DNA (probe DNA1), (c) sg-AuNPs with ds-DNA, (d) dsDNA with EcoRI. (B) Control measurements for assaying the cleavage specificity of EcoRI endonuclease: (a) bare sg-AuNPs, (b) sg-AuNPs with ss-DNA (probe DNA3), (c) sg-AuNPs with ds-DNA, (d) dsDNA with EcoRI, and (e) dsDNA with enzyme reaction buffer.

sg-AuNPs can be considered to be multiple tiny electrodes where the DNA strand can propagate electrons. Moreover, more compact π–π stacking in hybridized dsDNA could contribute to forming electron delocalization, so the double-stranded DNA provides additional electron tunneling path and has higher electric current than the signal-stranded DNA. As shown from curves b and c, the electric current difference between ssDNA and dsDNA can be observed clearly, which implies that the microelectrode with sg-AuNPs is quite suitable for DNA electrical detection.

3.3. Electrical detection of dsDNA cleavage by EcoRI

When the DNA strand can bridge the neighboring sg-AuNPs, dsDNA is detected directly by the *I–V* curve measurement. Further research of the microelectrode, which has sg-AuNPs and dsDNA, is the detection of some other biomolecules that have interactions with DNA. The simple and easy choice is EcoRI restriction endonuclease, which can recognize and bind to specific nucleotide sequences (5′-GAATTC-3′) resulting in cleavage of the DNA molecule. In this work, short dsDNA oligonucleotides were used as model DNA to study dsDNA cleavage by EcoRI. The motivation of this work is to propose a new approach to study DNA–protein interaction for research application.

I–V curves of sg-AuNPs with dsDNA and dsDNA with EcoRI are shown in Fig. 5A compared to the curves c and d. Thiolated probe DNA1 and complementary target DNA2 contain two recognition sequences for the EcoRI endonuclease. Hence the dsDNA formed by hybridization of DNA1 and DNA2 is cleaved at two specific sites and the electron tunneling path made by dsDNA is cut off completely. The electric current decreases after the sg-AuNPs with dsDNA treated with EcoRI for 5 min. The current magnitude of dsDNA with EcoRI is higher than bare sg-AuNPs and lower than sg-AuNPs with ssDNA (curves d, a and b).

In the present work, dsDNA cleavage by EcoRI is investigated real-time, which is monitored by detecting the change of *I–V* signals with the increasing time. Fig. 6 shows real-time *I–V* curves after digestion with EcoRI. The curves a and g represent *I–V* responses of sg-AuNPs with dsDNA and bare sg-AuNPs, respectively. After immersed in enzymatic cleavage mixture, the electric current decreased with the increasing time, indicating that EcoRI cleavage occurred. As seen from curve b to f, the electric current has a rapid decrease after adding EcoRI in the first 3 min (curves b, c and d), then the current decreases slowly as time lapsed and starts to level off above 5 min (curves e and f), indicating that dsDNA is cleaved by EcoRI after 5 min of enzyme reaction time. In order to prove that the decrease in electric current is a result of scission and not be affected by any other reasons, two control experiments were performed below.

As is well known, EcoRI is a site-specific endonuclease which recognizes the sequence GAATTC. To evaluate this, control probe DNA3 and target DNA4 were selected to assay the cleavage speci-

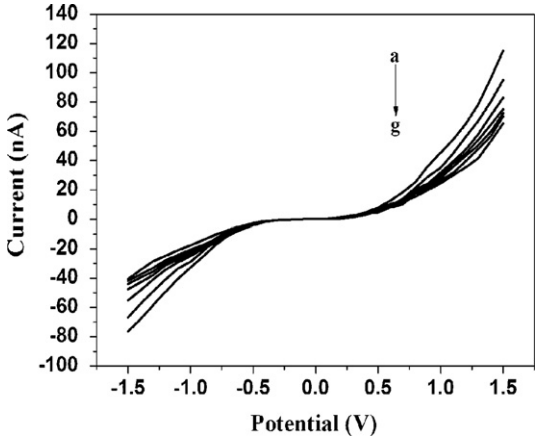

Fig. 6. *I–V* measurements for dsDNA cleavage by EcoRI at different reaction times: (a) 0, (b) 1 min, (c) 2 min, (d) 3 min, (e) 4 min, (f) 5 min, and (g) bare sg-AuNPs.

ficity of EcoRI endonuclease. DNA3 and DNA4 were designed as control DNA without specific recognization site of EcoRI endonuclease. Thiolated control probe DNA3 was immobilized on the surface of sg-AuNPs and hybridized with DNA4. As shown in Fig. 5B, the results of DNA immobilization and hybridization are in accordance with the results obtained above. However, the electric current does not decrease in the presence of EcoRI; furthermore, the magnitude and slope of the curves c and d are very close. That is, the electron tunneling path made by dsDNA is not cut off by EcoRI, suggesting that EcoRI has no effect on the DNA3 and DNA4 hybrid without containing specific recognition sequence for the EcoRI endonuclease. When the enzyme reaction buffer was placed on the dsDNA only, the electric current does not decrease and the magnitude and slope of the curves c and e are very close. It is concluded that enzyme buffer has no effect on electrical detection of dsDNA. From two control experiments, the decrease in conductivity is clearly suggested as a result of DNA scission.

4. Conclusions

In summary, a novel method for detecting the DNA hybridization and DNA–EcoRI interaction is demonstrated using the nanogapped AuNPs film by in situ seeding growth of AuNPs. The DNA strand served as a nanogap bridge provides an electron tunneling path between microelectrodes because of the appropriate distance between neighboring gold nanoparticles in comparison with the length of DNA. The sg-AuNPs microelectrode identifies dsDNA by *I–V* curve measurements when dsDNA is immobilized on the surface of sg-AuNPs after hybridization of the probe and target ssDNA. If dsDNA is cleaved by restriction endonuclease EcoRI, the electron tunneling path made by the DNA strand is cut off. The *I–V* curve change is used to characterize dsDNA–EcoRI interaction directly and the cleavage specificity has been investigated. The new method will be meaningful for the label-free detection of DNA–DNA and DNA–protein interactions, which builds up a new platform for studying biological processes. Finally, because this platform is based on one conventional microelectrode, it would become the DNA and protein biochips of massive multiplexing and high throughput through the use of large arrays of microelectrodes.

Acknowledgements

This work was partially supported by National Natural Science Foundation of China (60574095, 60711120174), National High Technology Research and Development Program of China (2006AA03Z309), the Young College Teachers' Research Fund Program of Anhui province (2007jql060zd) and the Knowledge Innovation Program of the Chinese Academy of Science (0723A15121).

References

[1] M.R. Arkin, E.D.A. Stemp, R.E. Holmlin, J.K. Barton, A. Hormann, E.J.C. Olson, P.F. Barbara, Science 273 (1996) 475.
[2] D.B. Hall, R.E. Holmlin, J.K. Barton, Nature 382 (1996) 731.
[3] I. Alexandre, S. Hamels, S. Dufour, J. Collet, N. Zammatteo, F. De Longueville, J.-L. Gala, J. Remacle, Anal. Biochem. 295 (2001) 1.
[4] M. Steichen, Y. Decrem, E. Godfroid, C. Buess-Herman, Biosens. Bioelectron. 22 (2007) 2237.
[5] V.C.H. Wu, S.H. Chen, C.S. Lin, Biosens. Bioelectron. 22 (2007) 2967.
[6] S. Roy, H. Vedala, A.D. Roy, D-h. Kim, M. Doud, K. Mathee, H-k. Shin, N. Shimamoto, V. Prasad, W. Choi, Nano Lett. 8 (2008) 26.
[7] B. Xu, P. Zhang, X. Li, N. Tao, Nano Lett. 4 (2004) 1105.
[8] D. Berdat, A.C.M. Rodríguez, F. Herrera, M.A.M. Gijs, Lab Chip 8 (2008) 302.
[9] J. Heitman, P. Model, Proteins 7 (1990) 185.
[10] M. Kurpiewski, L. Engler, L. Wozniak, A. Kobylanska, M. Koziolkiewicz, W. Stec, L. Jen-Jacobson, Structure 12 (2004) 1775.
[11] Y. Kim, J.C. Grable, R. Love, P.J. Greene, J.M. Rosenberg, Science 249 (1990) 1307.
[12] J. Hedgpeth, H.M. Goodman, H.W. Boyer, Proc. Natl. Acad. Sci. U.S.A. 80 (1972) 31.
[13] J.C. O'Brien, J.T. Stickney, M.D. Porter, J. Am. Chem. Soc. 122 (2000) 5004.
[14] Y. Weizmann, R. Elnathan, O. Lioubashevski, I. Willner, J. Am. Chem. Soc. 127 (2005) 12666.
[15] H. Watrob, W. Liu, Y. Chen, S.G. Bartlett, L. Jen-Jacobson, M.D. Barkley, Biochemistry 40 (2001) 683.
[16] B. Polisky, P. Greene, D. Garfin, B. Mcarthy, H. Goodman, H. Boyer, Proc. Natl. Acad. Sci. U.S.A. 72 (1975) 3310.
[17] Y. Jin, W. Lu, J.Q. Hu, X. Yao, J.H. Li, Electrochem. Commun. 9 (2007) 1086.
[18] A. Nitzan, M.A. Ratner, Science 300 (2003) 1384.
[19] K.W. Hipps, Science 294 (2001) 536.
[20] J.J. Storhoff, A.A. Lazarides, R.C. Mucic, C.A. Mirkin, R.L. Letsinger, G.C. Schatz, J. Am. Chem. Soc. 122 (2000) 4640.
[21] J.J. Storhoff, R. Elghanian, R.C. Mucic, C.A. Mirkin, R.L. Letsinger, J. Am. Chem. Soc. 120 (1998) 1959.
[22] B.M. Reinhard, S. Sheikholeslami, A. Mastroianni, A.P. Alivisatos, J. Liphardt, Proc. Natl. Acad. Sci. U.S.A. 104 (2007) 2667.
[23] S.J. Park, T.A. Taton, C.A. Mirkin, Science 295 (2002) 1503.
[24] H. Shiigi, S. Tokonami, H. Yakabe, T. Nagaoka, J. Am. Chem. Soc. 127 (2005) 3280.
[25] C.Y. Tsai, T.L. Chang, L.S. Kuo, P.H. Chen, Appl. Phys. Lett. 89 (2006) 203902.
[26] J. Turkevitch, P.C. Stevenson, J. Hillier, Discuss. Faraday Soc. 11 (1951) 55.
[27] G. Frens, Nat. Phys. Sci. 241 (1973) 20.
[28] K.R. Brown, M.J. Natan, Langmuir 14 (1998) 726.
[29] X.H. Yang, Q. Wang, K.M. Wang, W.H. Tan, H.M. Li, Biosens. Bioelectron. 22 (2007) 1106.
[30] I. Willner, F. Patolsky, Y. Weizmann, B. Willner, Talanta 56 (2002) 847.
[31] G. Festag, T. Schüler, R. Möller, A. Csáki, W. Fritzsche, Nanotechnology 19 (2008) 125303.
[32] E. Diessel, K. Grothe, H.M. Siebert, B.D. Waarner, J. Burmeister, Biosens. Bioelectron. 19 (2004) 1229.
[33] K.R. Brown, D.G. Walter, M.J. Natan, Chem. Mater. 12 (2000) 306.
[34] K.R. Brown, L.A. Lyon, A.P. Fox, B.D. Reiss, M.J. Natan, Chem. Mater. 12 (2000) 314.